6ICEGE 6th International Conference on Earthquake Geotechnical Engineering
1-4 November 2015
Christchurch. New Zealand

Structure-Soil-Structure Interaction Analysis in a Highly Seismic, Dense Urban Regeneration Zone

K. C. Ellison[1], A.M. Masroor[2], I. Almufti[3], M. Willford[4], N. O'Riordan[5]

ABSTRACT

Several structure-soil-structure interaction analyses were recently conducted using the finite element program LS-DYNA to assess the interaction between the deep, long embedded trainbox of the Transbay Transit Center and the adjacent deep basement of the 245-meter high 181 Fremont Tower when subjected to bedrock-propagating ground motions. Key features of this model, including the 181 Fremont basement and the soil domain, are removed from the SSSI framework in order to compare with the equivalent linear recommendations of NEHRP (2012) for the classical scenario of a basement embedded in an infinite soil domain. Discrepancies in the predictions of soil springs between the methods can largely be explained by the inability of the equivalent linear method to distinguish the significance of a thin, relatively soft clay layer immediately underlying the base mat. Good agreement is obtained for the spectral ratio between response spectra at the free field surface and base mat at periods greater than about 1.0 seconds. Finally, a soil-structure interaction analysis of the 181 Fremont Tower without the TTC is performed and compared with the results of the SSSI analysis. The presence of the TTC has a significant effect on the demands of the basement walls, diaphragms and drilled shafts.

Introduction

The Transbay Transit Center (TTC) under construction in downtown San Francisco will be the heart of a new urban redevelopment area (McLandrich, 2014). The TTC will function as a multi-nodal transportation hub, housing three above-ground levels including retail, bus terminals, and a roof park and two below-ground levels including a train station. The below-ground trainbox is a long, deep embedded structure approximately 17 m deep, 55 m wide, and 450 m long. The TTC is surrounded by existing structures and several new high rises with deep basements are planned or being constructed. The 245-meter-high 181 Fremont Tower will be the focus of the present study. It will be a state-of-the-art, mixed-use high-rise building to the south of the TTC with a 5-level, 19-meter-deep basement.

O'Riordan and Almufti (2014) examined the seismic stability of the braced TTC excavation adjacent to an existing tall building. More recently, the structure-soil-structure interaction (SSSI) effects between the 181 Fremont Tower deep basement, the TTC trainbox and other nearby high rises were assessed simultaneously for a suite of ground motions propagating from bedrock. The

[1]Senior Engineer, Geotechnics, Arup, San Francisco, CA, USA kirk.ellison@arup.com
[2]Engineer, Advanced Technology and Research, Arup, San Francisco, CA, USA, armin.masroor@arup.com
[3]Associate, Advanced Technology and Research, Arup, San Francisco, CA, USA, ibrahim.almufti@arup.com
[4]Arup Fellow, Advanced Technology and Research, Arup, San Francisco, CA, USA michael.willford@arup.com
[5]Arup Fellow, Geotechnics, Arup, London, UK, nick.oriordan@arup.com

extents of this model are presented in Figure 1(a). The corresponding idealized soil profiles along a slice to the south of the TTC are presented in Figure 1(c). In this paper, we compare the likely demands on the 181 Fremont basement from the aforementioned SSSI analysis with a soil-structure-interaction (SSI) analysis of the 181 Fremont Tower in an infinite soil domain. Both studies are performed using the finite element program LS-DYNA. In addition, the general applicability of LS-DYNA for this type of study is assessed by comparing the dynamic impedance (i.e., spring stiffness and damping) of the soil and embedment effects on the ground motions with the equivalent linear recommendations of NEHRP (2012).

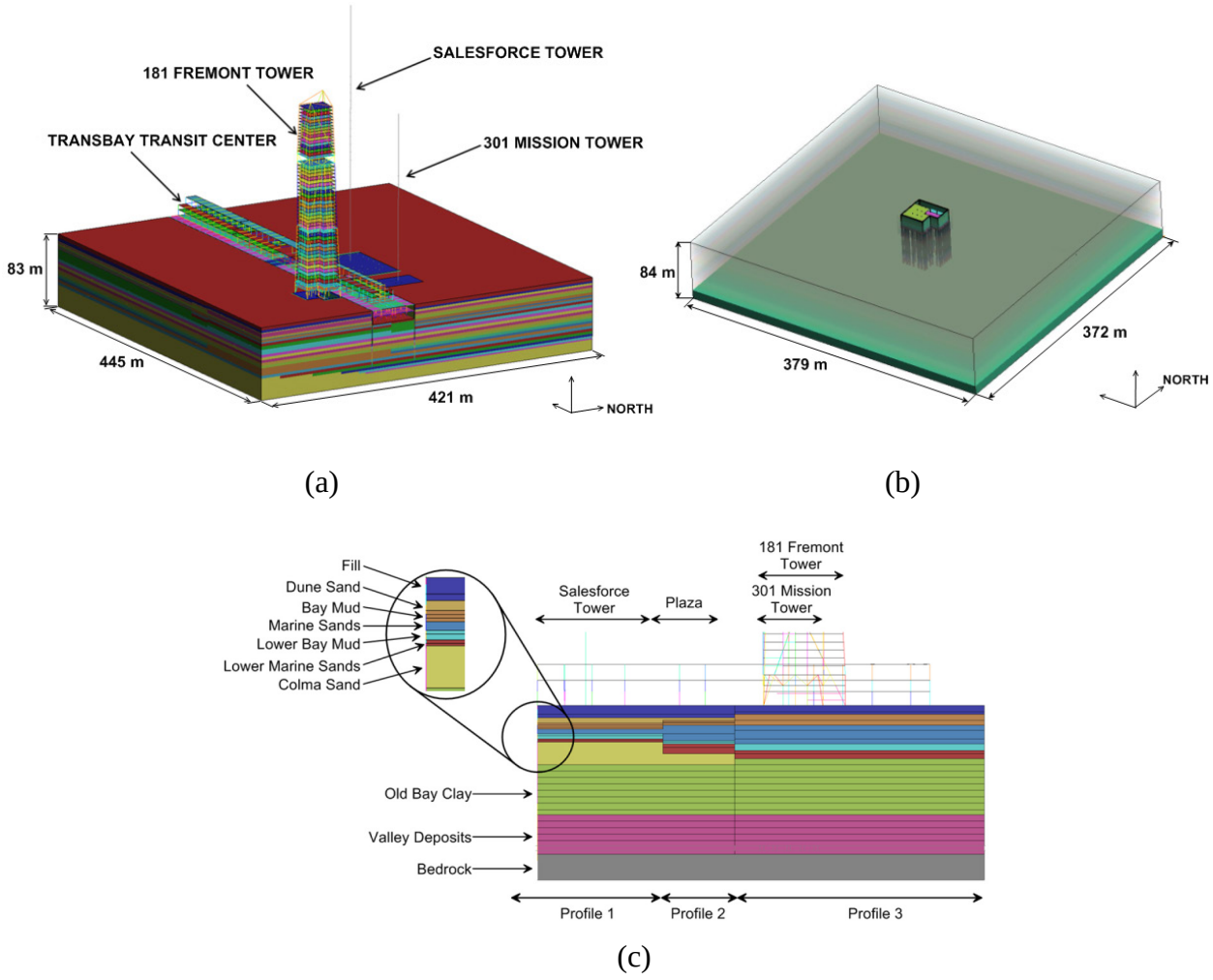

Figure 1. Views of the LS-DYNA models: (a) extents of model to capture structure-soil-structure-interaction effects, (b) extents of model to capture kinematic embedment effects, and (c) a northward looking slice along the south side of the TTC with soil parts recolored to indicate the idealized profiles

Characteristics of the Soil and Tower Structure

The basement footprint of the tower as modelled has major dimensions of 40.4 m by 37.2 m along the north and west edges, respectively, with a re-entrant southeast corner that is 10.9 m by

15.2 m. The foundation design includes 42 1.5- and 1.8-meter-diameter drilled shafts extending from the bottom of the basement (18.3 m) into the Franciscan Complex bedrock to a tip depth of approximately 79 m. A 2.4-meter-wide by 3.7-meter-deep pile cap surrounding the perimeter of the 0.9-meter-thick base mat caps 33 of the shafts. The remaining 10 shafts each underlie an interior column from the superstructure. The first and second modes of the structure are approximately 7.0 s and 2.5 s, respectively.

Figure 2(a) presents the idealized soil profile and shear wave velocity profile in the vicinity of the 181 Fremont Tower. This shear wave velocity profile is the main source of geotechnical input for the determination of dynamic stiffness and radiation damping for the soil-basement and soil-shaft interactions based on the recommendations of NEHRP (2012).

The finite element models in LS-DYNA explicitly capture the interaction between the soil and the 181 Fremont basement and foundation. The soil layers were modeled using the LS-DYNA material MAT_HYSTERETIC_SOIL. In this model, the shear strength and stiffness of the material is controlled by a nonlinear backbone curve comprised of 10 piecewise linear segments that scale with mean effective stress. The backbone curve was selected using the method of Yee et al. (2013) whereby the shear modulus degradation follows the recommendations of Darendeli (2001) up to a transition strain of approximately 0.1% and then smoothly transitions to approach a desired peak strength. Cyclic hysteretic behavior is governed by the Masing rule.

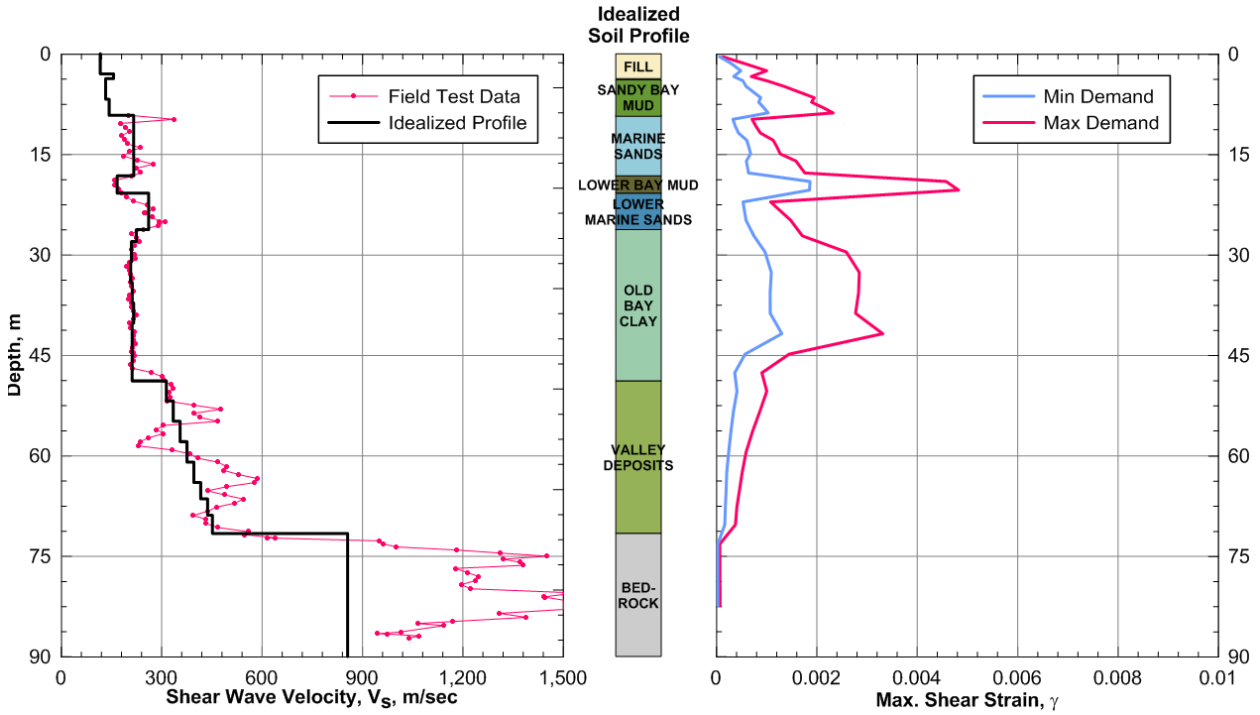

(a) (b)

Figure 2. Idealized soil profile including (a) shear wave velocity and (b) max shear strain mobilized during a sample 2D MCE level site response analysis

In the LS-DYNA models, the interface between the basement walls and the surrounding soil, is represented by a 1-element thick "disturbed" zone with reduced shear strength compared to the *in situ* material. The drilled shafts are represented by beam elements comprised of fiber integration points which enable plastic hinges to form if the demands exceed the capacity. They interact with the soil at their true diameter via springs which capture the side friction (t-z), end bearing (Q-z) and lateral (p-y) behavior.

Investigation of Equivalent Linear Impedance

Table 1 summarizes equivalent linear soil/shaft springs (Kx and Kxx) and dashpots (βx and βxx) computed for the first two modes of the 181 Fremont Tower using two different methods: 1) the NERHP (2012) approach; and 2) cyclic pushover analyses of the 181 Fremont basement and foundations embedded in an infinite soil domain. The model extents for the cyclic pushover analysis are shown in Figure 1(b).

The weight of the tower superstructure (approximately 320 MN) is applied as loads on the columns and walls of the basement in the pushover analyses, but the superstructure itself was not included. Vertical loads transferred to individual piles ranged from approximately 5 to 15 MN due to gravity. For the sake of comparison with the NEHRP (2012) approach, the basement is assumed to be perfectly rigid. In reality (and in subsequent simulations), the basement will have some flexibility since the ground level diaphragm is discontinuous on the side of the basement adjacent to the TTC.

Table 1. SSI springs for 181 Fremont basement

Method	**Location**	**2.5s Period**		**7s Period**	
		K_x (β_x)	**K_{xx} (β_{xx})**	**K_x (β_x)**	**K_{xx} (β_{xx})**
		(MN/m)	**(GN-m/rad)**	**(MN/m)**	**(GN-m/rad)**
NEHRP (2012)	*Basement*	*5,752 (36.2%)*	*3,528 (12.9%)*	*5,752 (17.6%)*	*3,673 (9.4%)*
	Bottom	3,766	1,480	3,766	1,543
	Sides	1,987	2,048	1,987	2,130
	Shafts	*10,322 (11.2%)*	*16,640 (12.7%)*	*10,324 (8.4%)*	*16,310 (10.1%)*
	Total	**16,074 (*21.8%*)**	**20,168 (*14.7%*)**	**16,077 (*13.4%*)**	**19,983 (*12.0%*)**
LS-DYNA	*Basement*	*12,163 (6.5%)*	*6,240 (3.6%)*	*11,442 (7.2%)*	*6,177 (4.0%)*
	Bottom	4,513	2,538	4,351	2,529
	Sides	7,650	3,702	7,091	3,647
	Shafts	*8,045 (3.9%)*	*11,652 (0.6%)*	*7,946 (3.6%)*	*11,662 (0.8%)*
	Total	**20,208 (*5.4%*)**	**17,893 (1.6%)**	**19,388 (*5.7%*)**	**17,839 (1.9%)**
Note: Damping values include radiation and material damping, where β_{soil}=8% for NEHRP (2012)					

In the first pushover analysis, a horizontal force of 60 MN is applied to the basement in sinusoidal cycles at frequencies of 0.143 and 0.4 Hz (i.e., periods of 7s and 2.5s, respectively). In the second pushover analysis, an overturning moment of 1000 MN-m is applied to the basement in sinusoidal cycles with the same frequencies. The magnitudes of the applied forces have been selected to approximately match the anticipated forces in the basement during a Maximum Considered Earthquake (MCE) level ground motion.

Due to the low frequency of the pushover analyses, a group efficiency factor of 0.6 is assumed for the shafts in the horizontal direction based on pseudostatic methods. This assumption is appropriate given that the dynamic stiffness components computed by the method of NEHRP (2012) are similar to their static values. A group efficiency factor of 0.4 is estimated for the shafts in the vertical direction based on the settlement observed in a gravity analysis.

A shear modulus ratio of G/G_0=0.40 was assumed for the computation of all compliance terms with the NEHRP (2012) method. This value was selected based on the max demand peak strains in Figure 2(b) mobilized during a sample MCE level site response analysis. The average shear modulus $G_{0,avg}$ used in the calculation of each term has been selected based on a depth of influence for the shear wave velocity Vs in accordance with the method.

A comparison of the springs computed by the NEHRP (2012) method and the springs computed by the pushover analyses reveals the following trends:

1) The proportion of K_x attributed to the bottom of the basement is low relative to the sides of the basement in the pushover analyses. This is because the base mat is underlain by a thin layer of Lower Bay Mud that is softer than other soil layers nearby. The NEHRP (2012) methodology smears the shear wave velocities to an assumed depth of influence of 37.2 m and therefore does not capture the significance of this softer zone.
2) The basement contributions to K_x and K_{xx} are lower for the NEHRP (2012) method than for the pushover analyses. In addition to the reason listed above, the NEHRP (2012) equations are based on Pais and Kausel (1988) and do not include corrections for the presence of bedrock at finite depth. An alternate elastic approach based on Roesset (1980) for an equivalent cylindrical foundation indicates that K_x and K_{xx} may be increased by approximately 50% and 25%, respectively due to the proximity of the bedrock.
3) The shaft contributions to K_x and K_{xx} are higher for the NEHRP (2012) method than the pushover analyses. In the NEHRP (2012) method, the total stiffness is obtained by summing the contributions of the basement and shafts without regard for possible interaction effects. However, it should be expected that the contribution of shaft springs would be reduced as the soil immediately underlying the basement will tend to displace with the base mat regardless of the presence of the shafts.
4) Lower damping was generally observed from the nonlinear pushover analyses. This was expected as damping is usually overestimated by equivalent linear methods. One reason is that the NEHRP (2012) method does not account for increasing shear modulus with depth. In addition, material damping may be underestimated in the LS-DYNA analyses

because of the piecewise linear nature of the modulus reduction curve and because small strain damping D_{min} was not included in the model.

Investigation of Kinematic Effects

The finite element model employed for the pushover analyses above has also been used to investigate the kinematic effect of the deep embedded basement on the ground motion at the base of the structure.

Sixty-six 2D bedrock ground motions have been developed for the site by the conditional mean spectrum (CMS) method, including 11 ground motions matched to periods of 2.0 s, 7.5 s and 10.0 s for both 475-year and MCE level events. The acceleration time histories are applied to the base of the finite element model in order to obtain equivalent acceleration time histories at the base mat. Figure 3(a) compares the bedrock, free field and base mat response spectra for the same MCE level event as in Figure 2(b). This ground motion corresponds to the 1980 Irpinia earthquake recorded at Bagnoli Irpinio station matched to the target spectrum at a period of 2.0s. It is a pulse-like motion.

Figure 3(b) compares the average spectral ratio between the free field and base mat response spectra for all 66 ground motions with the theoretical embedment effect predicted using the methodology of NEHRP (2012). Decent agreement is obtained at periods greater than about 1.0 s. The divergence between the theoretical and observed spectral ratios at higher frequencies likely results from rocking of the basement and the non-uniform nature of the soil profile.

The LS-DYNA model does not account for additional kinematic effects due to base slab averaging. In this case, the NEHRP (2012) approach indicates a slight reduction in spectral ratio of 3% and 0% for periods of 2.5s and 7s, respectively.

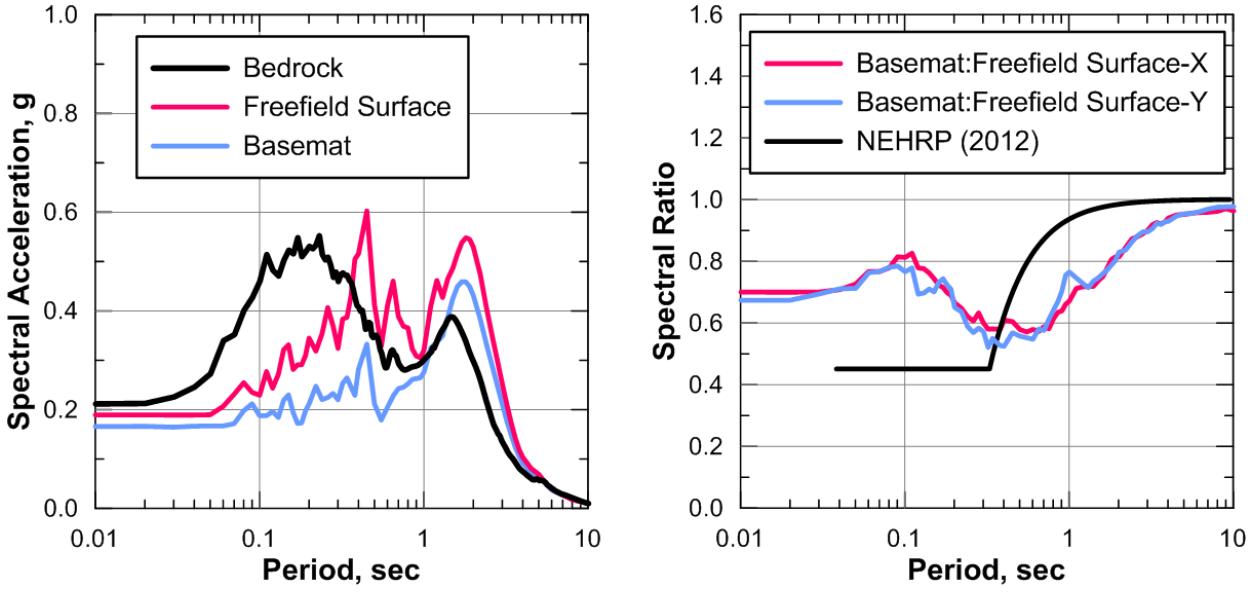

(a) (b)

Figure 3. Comparison of spectral acceleration between the free field surface and base mat for (a) a sample MCE level ground motion and (b) the average spectral ratio for all 66 ground motions

Comparison of SSI and SSSI Results

The primary purpose of the SSSI model was to examine the effects of the adjacent towers and deep basements on the TTC. As a result, the model includes the Salesforce Tower and 301 Mission Tower on the opposite side of the TTC in relation to the 181 Fremont Tower. The focus of the study herein is limited to the effect of the TTC on the 181 Fremont Tower. We have not assessed the extent to which the presence of the Salesforce Tower and 301 Mission Tower contribute to the observed behavior of the 181 Fremont Tower; however, we anticipate that their influence is not very significant in relation to that of the TTC.

Based on the geometry of the site there is an approximately 0.6-meter-thick “gap” between the TTC shoring wall and the 181 Fremont Tower basement wall that will be backfilled with concrete at the same time and with the same mix as the 181 Fremont basement wall. Thus, there is a direct structure to structure load path between the TTC trainbox and the 181 Fremont basement. In the finite element model, the concrete filled “gap” is not meshed with the shared shoring wall. Instead, they interact through a contact algorithm that does not transmit tensile forces and would enable the walls to separate, if necessary.

Figure 4(a) presents the normal forces on the 181 Fremont basement at two time instants corresponding to the maximum force on the pile cap and the maximum force near the top of the basement during the same MCE level ground motion shown in Figures 2(b) and 3(a). These stress concentrations are out of phase due to the rocking of the structures. The greatest stresses are concentrated at the following locations: 1) where the 181 Fremont pile cap meets the TTC base mat; 2) where the 181 Fremont level B2 diaphragm meets the TTC level B1 diaphragm at a depth of approximately 8 m; and 3) where the 181 Fremont transverse basement walls meet the TTC ground level diaphragm. For comparison, Figure 4(b) presents maximum normal stress envelopes acting on three vertical sections of the basement wall during the SSI analysis without the TTC.

Figure 5 presents shear forces through the 181 Fremont basement for both the SSI and SSSI analyses at time instants corresponding to the maximum positive shear at level B4, just above the pile cap. The figure also presents the instantaneous contact forces transmitted from the TTC. The magnitude of the shear force at level B4 is greater when the TTC is included. Tracking shear forces above and below the pile cap indicates that a significant portion of the shear force is resisted by the TTC base mat in the SSSI simulation, reducing the shear force in the positive direction transmitted to the soil and shafts below the base mat. However, the presence of the TTC increases
shear demands on the soil and shafts below the base mat in the negative direction where there is no adjacent structure to restrain the 181 Fremont basement.

Due to rocking, the peak shear forces in the 181 Fremont superstructure are out of phase with the peak shear forces at level B4 that were shown in Figure 5. Peak shear forces of 22.2 and 20.2 MN develop at the base of the superstructure in the SSI and SSSI simulations respectively. Thus, the presence of the TTC appears to have a smaller effect on the superstructure demands than on the basement demands.

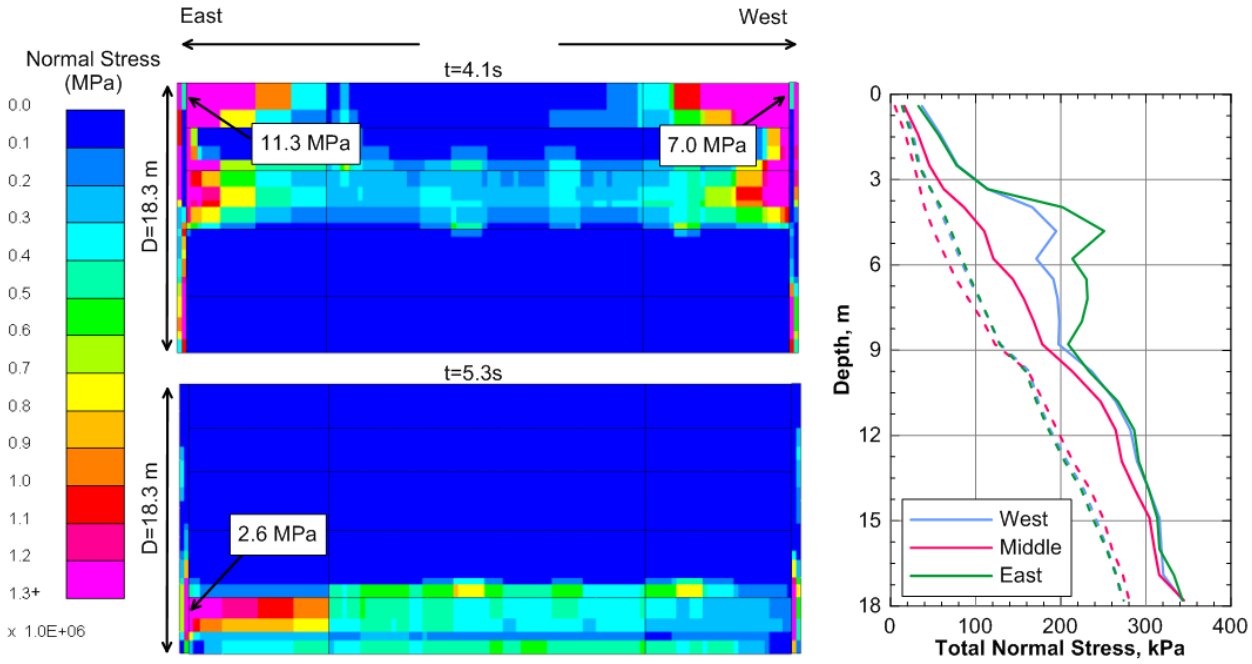

(a) (b)

Figure 4. Normal stress on the 181 Fremont basement wall (a) as contours at two time instants with the TTC modelled, and (b) as envelopes over the ground motion time history without the TTC modelled (note: dashed lines indicate the gravity-induced stresses).

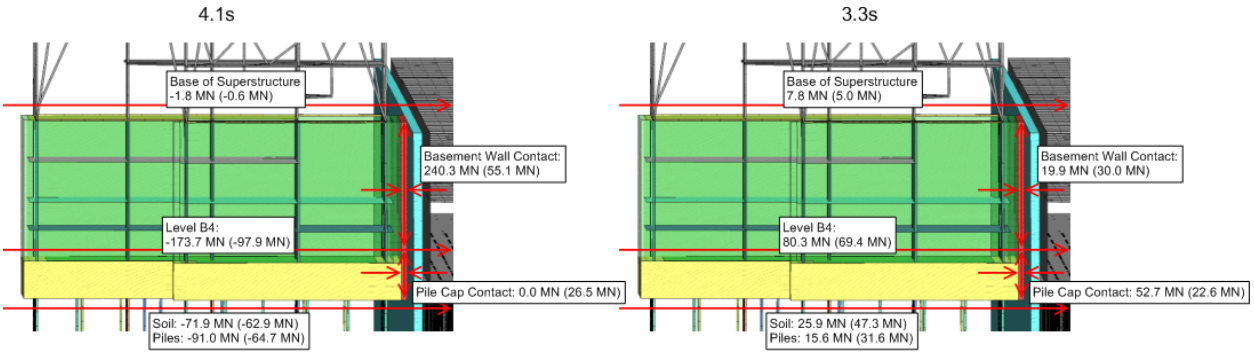

(a) (b)

Figure 5. Shear and contact forces in the 181 Fremont basement at the instant of (a) maximum negative shear, and (b) maximum positive shear at level B4 (note: values in parentheses are from the SSI analysis without the TTC)

Conclusions

The impedance and embedment effects of the 181 Fremont basement have been examined through simple equivalent linear methods based on NEHRP (2012) and nonlinear pushover analyses using the finite element program LS-DYNA. It is noted that the NEHRP (2012) method overestimated the contribution of friction along the bottom of the basement relative to the

passive force on the sides of the basement as it was unable to distinguish the significance of a thin, relatively soft layer of Lower Bay Mud underlying the base mat.

The kinematic embedment effect on reducing ground motions at the base mat has been examined by a large suite of analyses of the 181 Fremont basement subjected to a variety of ground motions propagating from bedrock. Decent agreement was generally obtained between the theoretical relationship in NEHRP (2012) and the relationship observed in the simulations above a period of about 1.0 seconds. The disparity at higher frequencies is likely due to a contribution from rocking of the basement.

Finally, the results of a soil-structure-interaction analysis of the tower and basement embedded in an infinite soil domain was compared with a structure-soil-structure interaction analysis including the Transbay Transit Center and other nearby high rises. The direct load path between the structures significantly affected the demands on the basement walls, diaphragms and shafts. The impact of the TTC on the demands of the 181 Fremont superstructure was less pronounced for this study. These findings highlight the importance of considering structure-soil-structure interaction effects in dense, urban areas.

Acknowledgments

The authors acknowledge Jay Paul Company, the developer of the 181 Fremont Tower, and the Transbay Joint Powers Authority, the owner of the Transbay Transit Center, for their support and permission to share results from the SSSI analysis. The authors also acknowledge Michael Givens for providing some guidance regarding the NEHRP (2012) methodology.

References

Darendeli M. Development of a new family of normalized modulus reduction and material damping curves. *Ph.D. Thesis*, Dept. of Civil Eng., Univ. of Texas, Austin, 2001.

McLandrich S. The Transbay Transit Center: Breaking New Ground in Urban Geotechnics. Geo-Strata. – Geoinstitute of ASCE, **18**(3), 22-26.

National Earthquake Hazards Recovery Program. *Soil-Structure Interaction for Building Structures*. NIST GCR 12-917-21, 2012.

O'Riordan N. & Almufti, I. *Seismic stability of braced excavations next to tall buildings*. Proceedings of the ICE – Geotechnical Engineering, 2014: **168**(1): 31-41.

Pais A., Kausel E. Approximate formulas for dynamic stiffnesses of rigid foundations. *Soil Dynamics and Earthquake Engineering*, 1988; **7** (4): 213-227.

Roesset J. M. Stiffness and Damping Coefficients of Foundations. *Proceedings of Session on Dynamic Response of Pile Foundations: Analytical Aspects*, ASCE National Convention, Florida, 1980; 1-30.

Yee E., Stewart J. P., & Tokimatsu, K. Elastic and Large-Strain Nonlinear Seismic Site Response Analysis of Vertical Array Recordings. *Journal of Geotechnical and Geoenvironmental Engineering*, 2013; **139**: 1789-1801.